



Title	Dynamics of Particle Patterns in Dissipative Systems : Splitting · Destruction · Scattering
Author(s)	Nishiura, Yasumasa
Citation	Sugaku expositions, 22(1), 37-55
Issue Date	2009-06
Doc URL	<a href="http://hdl.handle.net/2115/42600">http://hdl.handle.net/2115/42600</a>
Rights	First published in Sugaku Expositions in Vol. 22, Num. 1, 2009, published by the American Mathematical Society.
Type	article
File Information	nishiura_SE22.pdf



[Instructions for use](#)

DYNAMICS OF PARTICLE PATTERNS  
IN DISSIPATIVE SYSTEMS  
-SPLITTING · DESTRUCTION · SCATTERING-

YASUMASA NISHIURA

1. INTRODUCTION

One of the recent trends in pattern formation theory is to study the interrelation and transitions among various type of solutions based on a list of a special class of solutions relevant to the problem, which seems to be becoming an essential tool to understand complex dynamics. We illustrate this through the study of dynamics of particle-like patterns such as pulses and spots arising in reaction-diffusion systems. We are especially interested in the dynamics of

**“self-replication, self-destruction, and scattering  
via collision processes”**

and present the state of the art and give a perspective for future development. The reason why we shed light on those three processes is that a typical class of complex dynamics can be obtained as a combination of them. For instance, Figure 1 shows a spatio-temporal chaos for the Gray-Scott model (1) (GS model) and self-replication (splitting) and self-detruction (disappearance) of spots are observed there. Figure 2 shows a one-dimensional self-similar pattern in which annihilation occurs after collision between two pulses other than self-replication. We start the discussion by employing the GS model [5], [24] below, and treat other models in later sections including the FitzHugh-Nagumo model and the Gierer-Meinhardt model. Most of our results are, however, basically independent of the model systems, since our characterization of those dynamics is of a geometrical nature. The GS model takes the following form:

$$(1) \quad \begin{cases} \frac{\partial u}{\partial t} = D_u \Delta u - uv^2 + F(1 - u), \\ \frac{\partial v}{\partial t} = D_v \Delta v + uv^2 - (F + k)v, \end{cases}$$

which is one of the oxidation-reduction models describing the FIS-reaction ([14]), where  $u$  is a substrate,  $v$  is an activator,  $F$  and  $k$  are the parameters related to the inflow and removal rate of chemical species, and  $D_u$ ,  $D_v$  are diffusion coefficients.

Our problems are the following.

- (1) Find the underlying mechanisms causing self-replication and self-detruction, and how they are interwoven to produce the complex dynamics.

---

This article originally appeared in Japanese in *Sūgaku* 55 (2) (2003), 113–127.  
2000 *Mathematics Subject Classification*. Primary 37L10; Secondary 35K40, 35K55, 82C21.

- (2) Find the object which controls the scattering process among traveling pulses or spots.

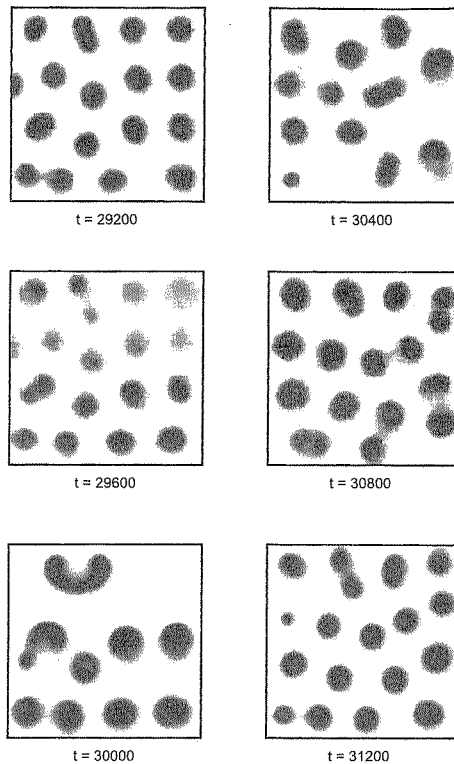


FIGURE 1. Two-dimensional spatio-temporal chaos for the Gray-Scott model. Each spot can replicate by itself. After the domain is filled by the spots, there occurs a competition searching for fresh substrate among them. The four spots in the top right start to disappear around  $t = 29600$  and vanish completely at  $t = 30000$ . The surrounding spots invade into the empty region and start to replicate there until the domain is filled by four islands again at  $t = 31200$ . Self-replication and self-destruction successively occur in a chaotic manner.

Ordered patterns are observed for a short time and locally in space as in Figure 1, which are of course transient and the orbit itinerate among such quasi-ordered patterns via splitting and destruction. What we are interested in is to clarify the underlying mathematical structure behind the scene which drives such a dynamics, for instance, how one spot can split into two spots and how annihilation or coalescence of two traveling pulses is controlled during the collision process as in Figure 8. Obviously such processes must be related to some instabilities or unstable objects; in fact, for the scattering case, highly unstable steady states as in Figure 8 and Figure 9 turn out to play a crucial role in understanding the scattering process between two colliding pulses. Difficulties encountered here are

- Large deformation of orbital profile.

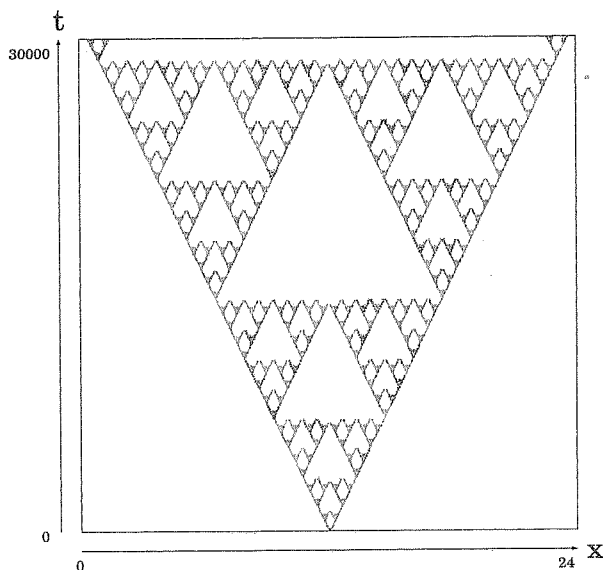


FIGURE 2. Spatio-temporal self-similar pattern for the Gray-Scott model (1) in which the  $v$ -component is shown in gray-scale. Self-replication and annihilation are balanced so that a Sierpinski-like self-similar pattern is produced. This was first found by Hayase-Ohta [10] for the reaction-diffusion system with the nonlinearity of Bonhoeffer-van der Pol type.

- Topological change such as number of pulses or spots.
- Detection of hidden highly unstable patterns.

There are no general theoretical tools powerful enough to solve all these issues; however conventional methods such as dynamical system theory, bifurcation, singular perturbation, and asymptotic methods give us partial (and local) answers to them. Our task is to do a patchwork combing all these clues and present a global geometrical perspective universal to vivid transient dynamics. The computational approach is at present the most powerful for our purpose; in particular, the global interrelation among various ordered solution branches becomes a key for the geometrical characterization, which can be obtained by using a pde-version of path-tracking software (such as AUTO [2]). Once such a geometrical characterization is obtained, it opens the way to get a general perspective to transient dynamics and even rigorous analysis. It turns out that the **hierarchical structure of saddle-node points** is responsible for self-replication and self-destruction, the **generalized heteroclinic orbit** is imbedded in the spatio-temporal chaos, and hidden saddles called **scatters** control the scattering process. The aim of this paper is to overview these results and suggest future directions for understanding the transient dynamics. As for a general reference, see, for instance, [20], [21], [22], [23]; one may consult the literature in each section for the details.

## 2. WEAK AND STRONG INTERACTIONS AMONG PARTICLE SOLUTIONS

Let us call a certain class of solutions an “object”, e.g., steady states, time-periodic solutions, traveling waves, chaotic patterns, etc. This is just a convention in this paper, and a class of spatially localized patterns is one example of an object. There are three stages in pattern formation theory.

- (1) Discovery of a new class of object.
- (2) Weak interaction among solutions in the object.
- (3) Strong interaction among solutions in the object.

The first stage is to explore and find various types of solutions by experiments and/or simulations and their stabilities, bifurcations and so on. Once a new model system is given, one may start from this stage. This is in some sense to make a list of “special functions” for a given model system. The second and third stages concern interactions among solutions in the object. Weak interaction means that the whole dynamic process can be well-approximated by making copies of solutions when they are isolated; namely, each participant keeps its identity and interacts only through tails. Very slow motion of 1D fronts and interactions among well-separated pulses, spots, and vortex are typical examples. A great advantage of this stage is that one can reduce the whole dynamics to a finite-dimensional ODE dynamics. Pulses and spots are regarded as points in space and the resulting ODE dynamics gets a universal form independent of the original model systems. The third stage, on the other hand, is quite different from the second one, and each pattern loses its identity, for instance, via strong collisions and undergoes a large deformation. Self-replication and self-destruction can be regarded as a strong interaction with itself. There are no general methods to handle this type of dynamics; however, the following three approaches and their combination seem to work for our purpose in a complementary way.

- **Weak interaction approach combined with singularities**
- **Elucidation of the global geometrical structure of solution branches that drives complex dynamics; a hidden hierarchy structure of solution branches**
- **Hidden saddles in scattering dynamics**

Physicists took the initiative in developing the weak interaction method among pulses such as [3] and [4], but it was rather recently that a rigorous base was given to it (see for instance [6]). The key assumption for this case is that each pattern is asymptotically stable when it is isolated. Our interests go beyond the case in which each localized pattern has some instabilities such as drifting, saddle-node, Hopf or their combination. The resulting dynamics becomes much richer even within the weak regime due to the instabilities, and the reduced ODE dynamics essentially takes a form of normal form of singularities plus weak interaction terms of exponential type (see, for instance, [7], [9]).

The second approach ([15], [16], [20], [21]) takes the viewpoint of how the whole structure of the set of solution branches drives the dynamics rather than just pursuing a specific branch. This is a tough task especially for PDEs; however, recent easy access to computational resources allows us to detect at least part of the big picture. In fact, self-replication (wave-splitting) and self-destruction of the wave train are basically caused by the same global bifurcational structure, i.e., tandem

structure of saddle-node points, although they look like reverse dynamics. Path-continuation software such as AUTO ([2]) is indispensable for this purpose, and this approach combined with the development of rigorous computer-aided proof and a topological approach ([11]) opens a way to new rigorous analysis in a variety of dynamics to which conventional methods cannot be directly applicable.

The third approach concerns the large deformation of particle-like patterns during the scattering process. A strong collision between two traveling objects destroys the original form of the waves and drives it to a distant place in phase space, and emits some output afterwards. The difficulty is to clarify the intermediate part of the whole scattering dynamics and detect a mathematical mechanism controlling the dynamics. It turns out that hidden saddles called **scatters**, which are highly unstable, play a crucial role for controlling input-output relation via large deformations. The diversity of outputs after collisions comes from the diverse directions of unstable manifolds of scatters and their heteroclinic connections.

### 3. SELF-REPLICATION AND SELF-DESTRUCTION

Particle patterns such as pulses and spots in dissipative systems make a sharp contrast with solitons in dispersive systems such as KdV and nonlinear Schrödinger equations; namely, there are no conservative quantities for dissipative particle patterns. Dissipative particles therefore can replicate or disappear by themselves, and when they collide, they annihilate or fuse into one body depending on the parameter values. We focus on the replication and destruction dynamics in this section. These two processes have opposite directions regarding the number of particles; however it turns out that the same mechanism called **hierarchy structure of saddle-node points** drives those dynamics. It should be noted that it does not matter what kind of solution forms each solution branch; what matters is the global interrelation among those branches.

First we take the following FitzHugh-Nagumo equations and consider the destruction process of multi-pulse waves as in Figure 3

$$(2) \quad \begin{cases} u_t = D_u u_{xx} + u(1-u)(u-a) - v, \\ v_t = \varepsilon(u - \gamma v). \end{cases}$$

The usual one-dimensional pulses of (2) have monotone tails and they are mutually repulsive (see, for instance, [21] and the reference therein). In order to have a stable multi-bump wave such as Figure 3, the local dynamics around the background state  $(0, 0)$  has to have an oscillatory nature; namely, its linearized equation, after getting on a moving coordinate, has a pair of complex eigenvalues. In fact, for a given  $n$ , this can be achieved by tuning the parameters  $a$  and  $\gamma$  and the resulting pulse has an oscillatory tail with  $n$  bumps (see, for instance, [3], [4]). For example, for  $\gamma = 2.0$  and  $a = 0.115$  with  $D_u = 0.00001$  and  $\varepsilon = 0.01$ ,  $n$ -multiple ( $n = 1, 2, 3, \dots$ ) pulses coexist depending on the initial data; however, when the parameter  $a$ , which controls the size of the threshold, is increased and fixed as  $a = 0.117$ , then each multiple pulse no more exists and the only asymptotic state is the trivial background. What we are interested in here is not just its asymptotic behavior, but the manner in which it collapses. The triple-pulse, for instance, does not break down at a stretch. The leading pulse first decays and disappears while the remaining two pulses keep almost their original shape; then the second one consecutively dies away in a similar way. It is not an easy task to describe the

detailed process of this collapse, partly because conventional analytical tools such as the comparison principle cannot be directly applicable.

Our strategy is that we look at all solution branches associated with these multiple-pulse waves and consider the geometrical interrelation among them. In fact the first three branches corresponding to an  $n$ -multiple pulse can be computed by path-continuation method as in Figure 4 with  $a$  being the bifurcation parameter. A remarkable thing is that the location of saddle-node point of each branch almost coincides numerically; therefore the onset of collapse of an  $n$ -multiple pulse occurs (almost) simultaneously. Such a structure is called the **hierarchy structure of saddle-node points** and plays a key role in the sequel. The reason for successive collapse is attributable to the presence of saddle-node points and the connecting manner of their unstable manifolds. More precisely the vector field near the SN-point is close to zero; therefore the time evolution is slow if the solution profile is close to that of the SN-point (the “aftereffect” of the SN-point). Moreover, the destination of the unstable manifolds starting from the lower branch of the saddle-node singularity for the  $n$ -pulse is the stable part of the  $(n - 1)$ -pulse. These observations are obtained numerically; however they strongly suggest that singularities and global geometrical interrelations among solution branches drive the self-destruction process. It should be noted that there are no ordered patterns in the phase space at the parameter values where we observe successive destruction of pulses, although the orbits pass by the saddle-node points. From the asymptotic viewpoint, the number of humps is decreasing and the orbit eventually goes to the trivial background state; however, we are interested in the transient dynamics that the orbit visits at the quasi- $n$ -pulse for certain successive durations, which is driven by the above hierarchy structure of SN-points and the onset of such a destruction process is given by the location of the SN-point.

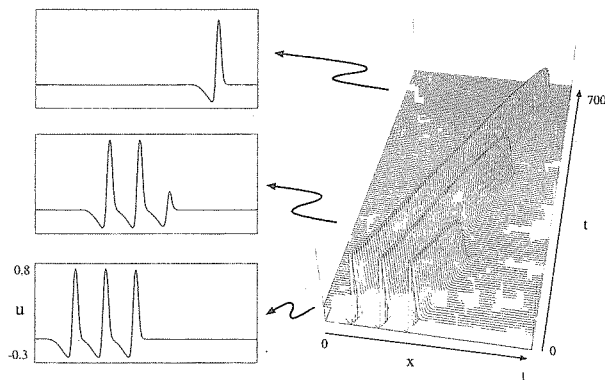


FIGURE 3. Self-destruction of triple-traveling-pulse oscillatory tail.

The opposite direction of dynamics **self-replication** is caused by a similar hierarchy structure of SN-points. The difference is its connecting manner of unstable manifolds; namely, the unstable manifold of the  $n$ -th hump pattern is connected to the  $m$ -th one where  $m > n$ . The number of humps is increasing and the final pattern in a bounded domain is typically a spatially periodic state (Turing pattern). The relation between  $n$  and  $m$  is rather delicate and depends on the boundary conditions; however, it can be shown that  $m = n + 2$  in 1D extended domains: namely,

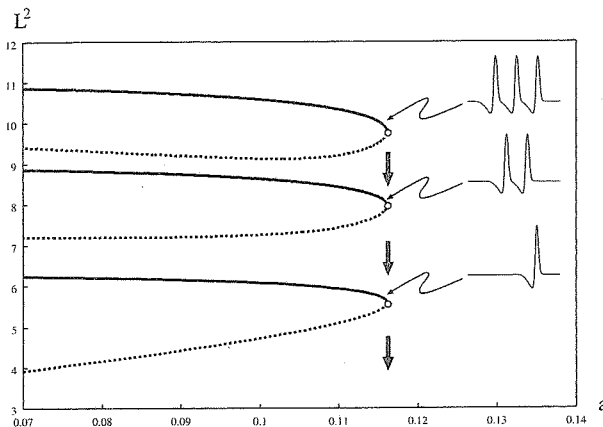


FIGURE 4. Global bifurcation diagram for the self-destruction process of a triple-traveling-pulse with an oscillatory tail. The horizontal axis is the threshold parameter  $a$  and the vertical axis is the  $L^2$ -norm of the solution. The locations of single, double and triple pulses coincide with each other with high accuracy. Successive destruction occurs in the right part of this location.

the only two pulses located at an edge can replicate and the remaining ones do not. We will discuss this later.

This geometrical characterization indicates that once a model system has such a hierarchy structure and connecting properties of unstable manifolds, it has a potential to drive self-replication.

In fact the following Gierer-Meinhardt model (3) also has self-replication dynamics in a similar way to the well-known Gray-Scott model (see, for instance, [14], [15], [24]):

$$(3) \quad \begin{cases} a_t = \epsilon^2 \Delta a - a + \frac{a^2}{h}, \\ \epsilon^2 h_t = \Delta h - \mu \epsilon^2 h + a^2. \end{cases}$$

The replicating dynamics of (3) and the associated global bifurcation diagram are given by Figure 5 in which the hierarchy structure of SN-points is clearly visible. The distance between newly born pulses gradually increases and only the pulses located at both ends can replicate by themselves; namely, the increasing manner is not like  $2^n$ :  $\rightarrow 2 \rightarrow 4 \rightarrow \dots$ , but  $\rightarrow 2 \rightarrow 4 \rightarrow 6$ . In view of Figure 5, one may regard the self-replicating pattern as an expanding wave inside of which a cluster of periodic steady states is successively formed.

Employing the pulse-interaction method, which allows us to reduce the PDE dynamics to ODE dynamics, we can prove the above **edge-splitting** in the sense that the largest initial dimple-deformation in the middle of the pulse, which actually indicates the onset of splitting, is attained only at pulses located at an edge ([9]).

The resulting ODEs for  $N + 1$  pulses are given by

$$(4) \quad \begin{cases} \dot{h}_1 &= -M_0(e^{-\alpha h_2} - 2e^{-\alpha h_1}), \\ \dot{h}_j &= -M_0(e^{-\alpha h_{j-1}} - 2e^{-\alpha h_j} + e^{-\alpha h_{j+1}}), \\ \dot{h}_N &= -M_0(e^{-\alpha h_{N-1}} - 2e^{-\alpha h_N}), \\ \dot{r}_0 &= M_1 r_0^2 - \epsilon M_2 - M_3 e^{-\alpha h_1}, \\ \dot{r}_j &= M_1 r_j^2 - \epsilon M_2 - M_3(e^{-\alpha h_{j+1}} + e^{-\alpha h_j}), \\ \dot{r}_N &= M_1 r_N^2 - \epsilon M_2 - M_3 e^{-\alpha h_N}, \end{cases}$$

where  $r_j$  ( $j = 0, \dots, N$ ) stands for the depth of the dimple of each pulse,  $h_j$  ( $j = 1, \dots, N$ ) for the distance between the pulses, and  $\epsilon$  is signed distance from the location of the SN-point. All the coefficients  $M_j$  become positive for (3) and the equation for translation of the system is omitted here for simplicity. The equations for  $h_j$  are split from those of  $r_j$ ; therefore they can be analysed separately and they are basically mutually repulsive thanks to  $M_j > 0$ . Whether the pulse starts to split or not depends on the dimple-size of  $r_i$  and if it exceeds the critical size, then it starts to split into two pulses. Therefore it is important to know the location of those pulses that have the largest dimple-size. In view of the equations for  $r_j$ , it has a quadratic nonlinearity of  $r_j$  for fixed  $\epsilon$ ,  $h_j$  and when the intercept of its parabola becomes positive,  $r_j$  starts to increase. The issue is therefore reduced to finding which intercept becomes positive primarily, which is equivalent to detecting the largest  $h_j$  because the intercept term depends only on  $h_j$ . It is shown in [9] that  $h_1$  and  $h_N$  primarily reach the critical distance, and therefore we observe **edge-splitting**. The **critical distance** can be computed and has the order  $-\log|\epsilon|$ .

#### 4. SELF-REPLICATION AND SELF-DESTRUCTION CAN PRODUCE SPATIO-TEMPORAL CHAOS

One may naively expect that self-replication combined with self-destruction can produce a never-ending dynamics without settling down to a specific state; however, it is not so easy to achieve this task. Let us recall the self-destruction process as in Figure 3. The destination of the dynamics is the trivial background state and once the orbit falls into it, it never comes up again. Some sort of revival from the destruction state is necessary to create a birth-death circle. In order to revitalize the destroyed homogeneous state, say call it  $P$ ,  $P$  must have unstable directions, but at the same time  $P$  is the destination via the destruction process. In order to overcome this dilemma, we resort to the second approach in §2, namely to find all the relevant branches of patterns and extract a hidden driving mechanism. We already see such a spatio-temporal chaos in Figure 1; however, the 2D-case is difficult to handle at present, and hence we restrict ourselves to the 1D-case of the Gray-Scott model (1). We can find a similar spatio-temporal chaos as in Figure 6, which shows a cycle that itinerates quasi-ordered patterns and the homogeneous state via destruction. More precisely when we observe the dynamics of Figure 6 through a subinterval, we notice that there is a dynamic cycle consisting of the following four stages starting from the background state  $(1, 0)$ .

- (1) Creation of a spatially periodic pattern via a self-replication process from the homogeneous state  $(1, 0)$  with perturbation of finite size.
- (2) Temporal stay at the spatially periodic pattern.
- (3) Destruction to the homogeneous state  $P$ .

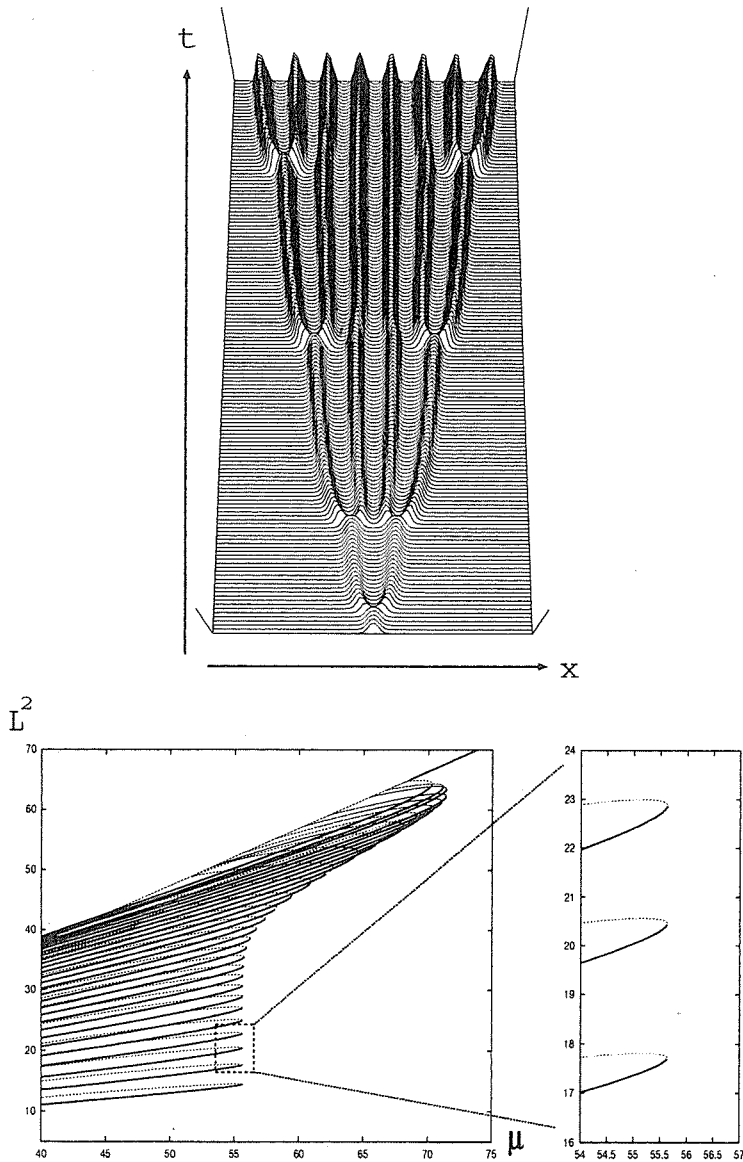


FIGURE 5. Self-replication dynamics for the Gierer-Meinhardt model. The upper picture shows the time-evolution of the replication process starting from a localized initial data. The global bifurcation diagram (below) with respect to the decay rate  $\mu$  shows the locations of saddle-node points for steady states of multi-hump type. The number of humps is increased from the bottom up. When the distance between humps is well-separated (i.e., lower branches), their locations coincide well; however, they don't coincide for higher modes due to the finite-size effect.

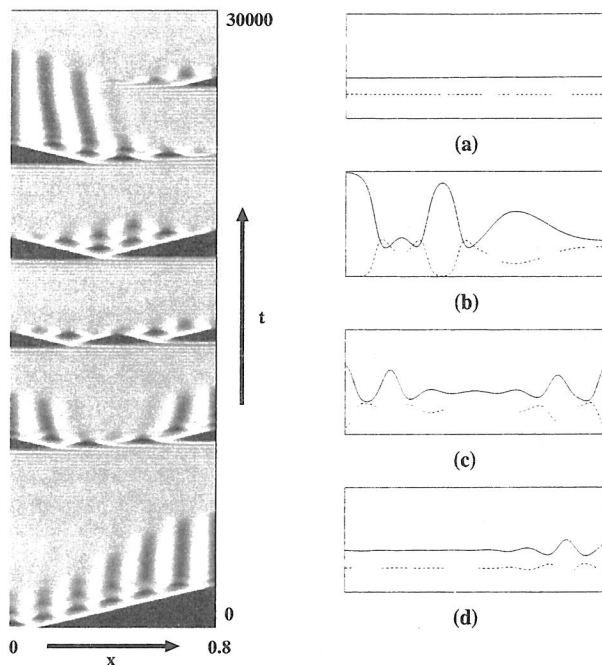


FIGURE 6. One-dimensional spatio-temporal chaos for the Gray-Scott model (gray-scale left) and typical profiles of  $u$  (solid line) and  $v$  (dotted line). It shows one cycle from an almost uniform state (a) to more or less the same state (d) via replication (b) and destruction (c).

(4) Non-uniform reentrant to  $(1, 0)$  along the unstable manifold of  $P$ .

The constant state  $P$  is another homogeneous equilibrium of the Gray-Scott model and Figure 7 presents a schematic picture of this loop structure. The first stage is a self-replication process triggered by the localized perturbation to  $(1, 0)$ . The second stage is the aftereffect of the SN-point associated with the periodic pattern and the third stage is its destruction process to  $P$ . If we can make the reentry from  $P$  to  $(1, 0)$  successfully, the whole dynamic cycle may run seamlessly. Note that reentrant to  $(1, 0)$  does not mean that the orbit falls into there uniformly (if so, it remains there forever, since  $(1, 0)$  is asymptotically stable in the PDE sense) and this non-uniformity originates from the nature of the instability of  $P$ .

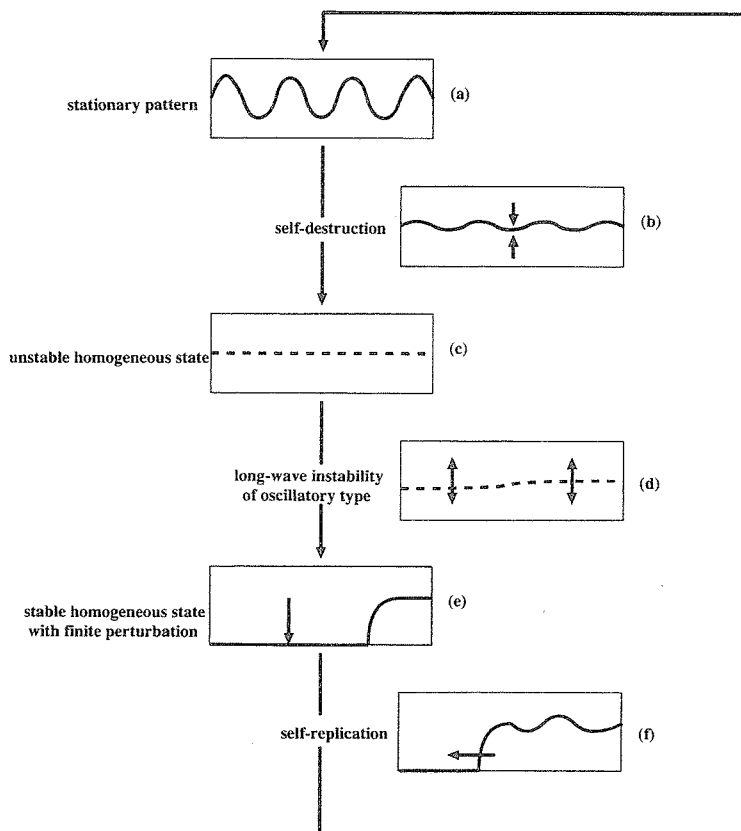


FIGURE 7. A generalized heteroclinic cycle for the Gray-Scott model. It consists of a spatially periodic pattern, an unstable constant solution  $P$ , and a stable constant state  $(u, v) = (1, 0)$  with localized perturbation. In a loose sense the orbit iterates these patterns when the system size is large enough. More precisely a self-replication wave starts from a localized perturbation and forms a periodic pattern; however, it destructs to the homogeneous state  $P$ . The constant state has an oscillatory instability of long-wave type, the destination of this instability is the background state  $(1, 0)$ , but it converges non-uniformly due to the oscillatory nature; therefore there always exists a localized bump as in (e) other than the  $(1, 0)$ -state, which is the beginning of another cycle.

It is easy to see via linearization that  $P$  has a long-wave oscillatory instability (see Figure 14 of [16]), and hence any spatio-periodic structure around it with medium or short wave-length collapses to it along its stable manifold. The quasi-periodic pattern at the second stage, which is not a long wave, is therefore close to the stable manifold of  $P$  and approaches it, i.e., destruction occurs. Since  $P$  is a saddle, after staying around it for a certain time, the orbit starts to leave there in an oscillatory manner. Recalling that the unstable manifold of  $P$  is connected to  $(1, 0)$  in the ODE sense, one may expect that the orbit eventually falls into  $(1, 0)$  and

nothing happens after that. In fact it could happen depending on the system size; however, if the system size is large enough so that long-wave instability of oscillatory type causes non-uniform convergence to  $(1, 0)$ , then a self-replication wave starts to propagate from the region away from  $(1, 0)$ . The issue is whether we could tune the parameters so that all these things occur simultaneously, in other words, to detect a sort of generalized heteroclinic cycle as in Figure 7. This is obviously related to the interrelation among global branches of periodic structure, homogeneous states  $P$ , and the background state  $(1, 0)$ . The second approach mentioned in Section 1 plays a crucial role in clarifying the situation and the locations of SN-points for periodic structures, and the Hopf-point of  $P$  turns out to control the onset of spatio-temporal chaos. See [16], [22] for detailed discussions.

## 5. COLLISION OF PARTICLE-LIKE PATTERNS

We have considered so far the dynamics of pulses driven by the intrinsic instabilities such as splitting and destruction due to the hierarchical saddle-node singularities. We shall study in the sequel another category of dynamics driven by the extrinsic forces. Here “extrinsic” means, for instance, heterogeneity of the media or interactions with other localized patterns. In this section we focus on the latter one, especially strong collisions between two traveling pulses or spots for the Gray-Scott model and the three-component reaction-diffusion system (5) arising in gas-discharge phenomena, i.e., scattering among particle patterns in dissipative systems. The velocity of the traveling pulse or spot in dissipative systems can be altered and controlled by varying kinetic parameters or diffusivities, and the collision process is changed drastically depending on the velocity. In fact, when the velocity is small, one can show that they interact weakly and repel each other like elastic balls [7], [8], although the angle of incidence is in general different from that of reflection; however, if the velocity is increased, then the output after collision is diversified such as annihilation, coalescence into one body, and splitting into many spots depending on the parameters [13], [1], [12], [17], [18], [19]. A natural question is “What is the underlying mechanism which controls and produces such a variety of outputs?”. The strong collision obviously causes a large deformation of profiles and it is not a priori clear in which basin the orbit falls after interaction. The final destinations nevertheless are in most cases either a combination of traveling patterns or homogeneous states (annihilation). One can imagine that if the orbit moves from one attractor to another, then it may pass by saddle points. The question is how we can find such unstable objects, if any, in a systematic way. In what follows we restrict ourselves to the head-on collision case and assume that initial data is given by the two traveling pulses or spots located at  $\pm$  infinity. For later convenience, we call such solutions of saddle type **scatters** (see [17] and [18]). Time-evolution itself does not directly give any hint about scatters, since those are in general highly unstable; however, there is a chance to detect a scatter near the critical parameter value at which the input-output relation changes qualitatively, say from reflection to annihilation. In other words, typically as in the codim 1 case, the orbit crosses transversally the stable manifold of the scatter when such a qualitative change occurs; i.e., the orbit takes a different route from the previous one among unstable directions. In general the codimension of the scatter is greater than 1, and therefore it demands a wider search in parameter space. Once scatters

are identified, the local dynamics of them shows how the orbits are sorted out depending on the parameters and allows us to classify and predict the input-output relations. Scatters are at present obtained only numerically; however, the singular perturbation method, for instance, can be applied to construct them rigorously once their precise profiles are clarified numerically.

In order to illustrate the idea of scatter, we first consider the transition from reflection to annihilation for the one-dimensional Gray-Scott model (1).

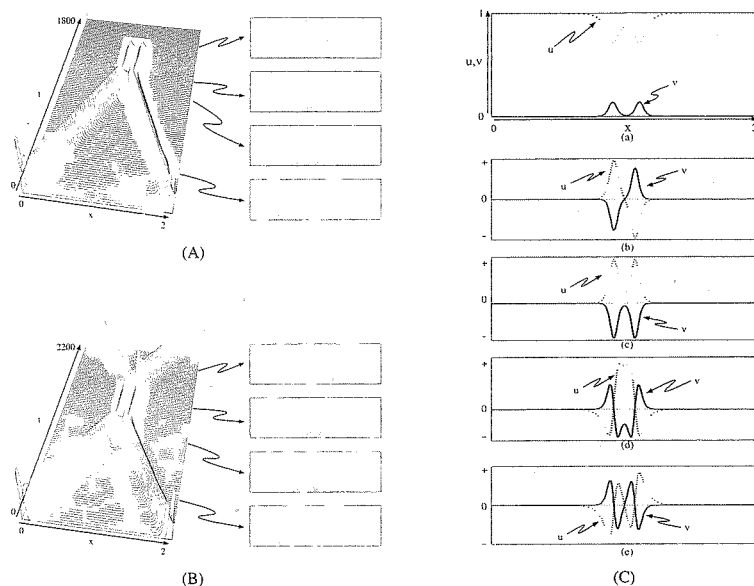


FIGURE 8. Scatter for reflection-annihilation transition and the associated eigenfunctions. As  $k$  is increased, the output is changed from annihilation (A) to reflection (B). Since both cases are very close to the transition point  $k_c$ , the profiles right after collision resemble the unstable steady state of twin-horn type depicted at the top of (C), called the twin-horn scatter. The linearized spectrum around it has three unstable eigenvalues besides the zero eigenvalue coming from translation invariance; i.e., their real parts are positive and the associated eigenfunctions are given as (a)-(c). The second symmetric case (b) plays a key role for head-on collisions.

**From reflection to annihilation.** As was mentioned before, the standing pulses of the Gray-Scott model repel each other, which strongly suggests that slow traveling pulses also repel each other. In fact this is the case [7] under certain conditions and agrees with the intuition that the inertia (kinetic energy) of the pulse cannot overcome the barrier of repulsive potential. The profiles of the solution become almost symmetric in the middle when the distance between two pulses becomes a minimum, and they change their directions smoothly without strong interaction. However, as  $k$  is decreased, the velocity is increased, two pulses interact strongly and it starts to **annihilate** when  $k$  becomes below a critical value

$k_c$ . Figure 8 shows their behaviors near  $k_c$ : two pulses are distorted and merge into one body and the new counter-propagating pulses are created for  $k > k_c$  or they annihilate after all for  $k < k_c$ . Here if we take a closer look at the deformation process at a collision point, the two solution profiles just before emitting the outputs are quite similar for  $k > k_c$  and  $k < k_c$  like a twin-horn structure (see Figure 8). The solution deforms slowly around the twin-horn shape and then decides the direction to go. The transient state of the twin-horn shape plays like a separator and can be detected via the Newton method as in 8(C)(a), which is an example of **scatters**. The linearized spectrum around the twin-horn scattor has three unstable eigenvalues besides the translation free zero eigenvalue (see Figure 8(C)) listing according to the size of the real parts in descending order. As far as head-on collisions are concerned, the second unstable eigenfunction plays a dominant role. In fact, by adding a tiny perturbation proportional to it, the output is either two counter-propagating pulses or annihilation depending on the sign of the perturbation, which makes the twin-horn scattor deserve to be called scattor, i.e., the scattor makes a traffic control at a collision point.

**Scattering process itinerating two scatters.** The following 3-component model was proposed as a qualitative model system describing the gas-discharge phenomenon ([1], [25]), which is known to have stable traveling spots in 2D and 3D space:

$$(5) \quad \begin{cases} u_t = D_u \Delta u + 2u - u^3 - \kappa_3 v - \kappa_4 w + \kappa_1, \\ \tau v_t = D_v \Delta v + u - v, \\ \theta w_t = D_w \Delta w + u - w. \end{cases}$$

The scattering process usually consists of multiple-stage dynamics which indicates that several unstable patterns become involved in the process of collision dynamics. We shall present a concrete example of such a multiple-stage process through the model system (5).

Typical input-output relations as well as bifurcation diagrams of standing and traveling pulses with respect to  $\tau$  are schematically depicted in Figure 9(A). The drift bifurcation from standing to traveling pulses occurs at  $\tau^d \approx 9.7$  supercritically. The interaction between standing pulses is of repulsive type; therefore it is inherited from the slow traveling pulses near the drift bifurcation point as in Figure 9 (bottom left in (A)). As  $\tau$  is increased, however, the input-output relation changes from two-pulse emission to one-pulse emission around  $\tau^s \approx 16.1328079$ . More noteworthy is that two scatters (unstable steady states) participate in the collision process (see Figure 9(B)): one is the twin-horn pattern of codim 3, which is similar to the one for the Gray-Scott model in Figure 8, and the other is the single-horn pattern of codim 1. When  $\tau$  is slightly smaller than  $\tau^s$ , the orbit approaches the twin-horn pattern and stays near it for a certain time, but the middle part of the twin-horn scattor starts to sink and it eventually splits into two counter-propagating waves. On the other hand, as  $\tau$  becomes slightly larger than  $\tau^s$ , after approaching the twin-horn scattor, its middle part starts to grow and almost looks like the single-horn pattern (see the magnified evolution in Figure 9(B)(a)). The single-horn scattor is, however, unstable to translational perturbation for  $\tau > \tau^d$ , and it eventually deforms into a traveling pulse. The orbit visits two scatters during the collision process like an orienteering. The twin-horn scattor has three unstable eigenvalues:  $\lambda_1 = 0.9069 > \lambda_2 = 0.1297 > \lambda_3 = 0.0138$ , and the first one is much larger than the remaining ones and dominates the dynamics around it. The associated

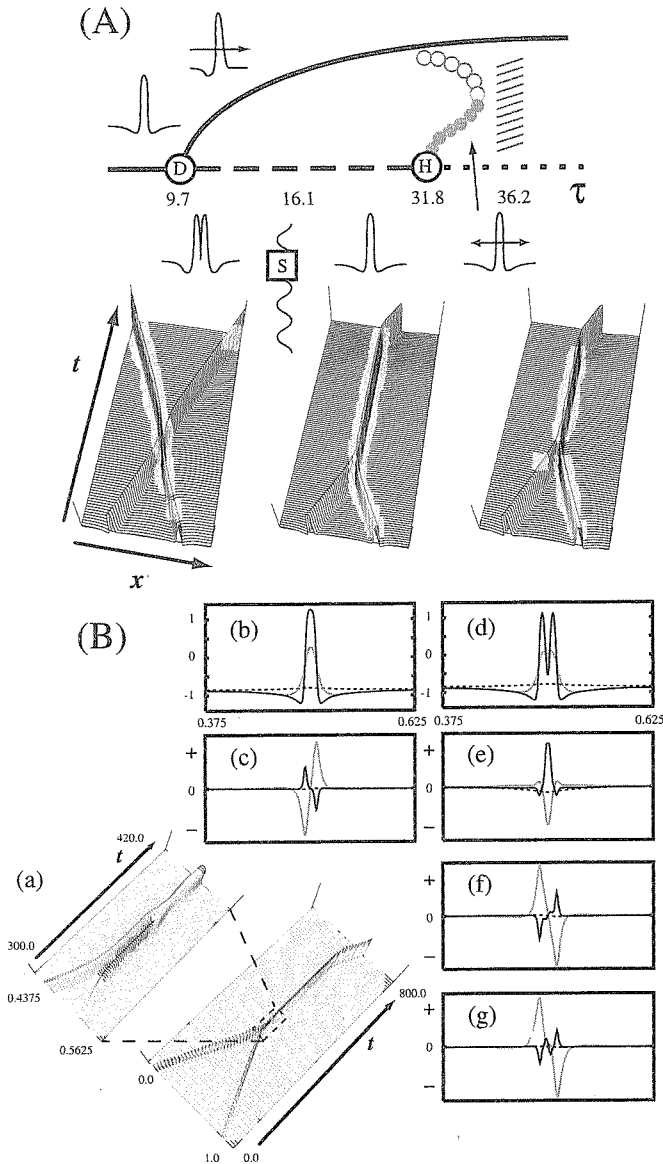


FIGURE 9. (A) Phase-diagram of scattering for the gas-discharge model. The three evolutions show 2 into 2 (reflection), 2 into 1 (coalescence) and 2 into 1 (coalescence with oscillation) (left:  $\tau = 15.0$ , center:  $\tau = 20.0$ , right:  $\tau = 35.0$ ) respectively. (B) Two scatterers and their heteroclinic connection: (a) When  $\tau$  is slightly larger than  $\tau^s$ , the orbit deforms along the heteroclinic connection from twin-horn scatterer to single-horn one. (b), (c) Single-horn scatterer and its unstable eigen-profiles. (d), (e)-(g) Twin-horn scatterer and its three unstable eigen-profiles. The solid (gray, dotted) line shows the  $u$ -component ( $v$ -component,  $w$ -component) respectively.

eigenfunction with  $\lambda_1$  has reflection-symmetry and has a sharp peak in the middle which is responsible for splitting into two pulses or merging into one pulse around  $\tau^s$ .

As  $\tau$  is increased more, it seems that there does not occur any qualitative change for input-output relations; however, if we take a closer look at the behaviors of the single-horn scattor, it oscillates in time as in Figure 9 (bottom right in (A)). This is because the single-horn scattor undergoes a supercritical Hopf bifurcation at  $\tau \approx 31.8$  which still keeps a drift instability. Note that if the head-on collision is perfectly symmetric, then the orbit should remain in the single-horn scattor; however, due to a tiny fluctuation, it eventually starts to move either to the right or left as a traveling pulse. The above observation clearly shows a **heteroclinic connection** from the twin-horn scattor to the single-horn one and the orbits are sorted out according to the initial deviations from a perfect-shaped pulse as well as the parameters.

Exactly the same scattering process has been observed also for two-dimensional traveling spots [18], [19]. Standing spots are stable for small  $\tau$ ; however, as  $\tau$  is increased, there occurs a drift bifurcation at  $\tau \approx 28.8$  and they start to move with constant velocity. Such stable traveling spots remain stable up to  $\tau \approx 94.0$ . Here we only consider head-on collisions. Two traveling spots bounce back near the drift bifurcation point. As  $\tau$  is increased, they merge into one body and it transforms into a traveling spot; namely, there is a transition from reflection to fusion with drift instability. Figure 10(A) shows an evolution of two colliding spots when  $\tau$  is slightly above the transition point  $\tau^s \approx 69.54853$ . The orbit first approaches the unstable steady state of peanut shape (Figure 10(A) below left), then the middle part of it grows up and becomes very close to another unstable steady state of single-horn type (Figure 10(A) above right). It stays near the single-horn shape for a certain time, then it deforms into a single traveling spot. On the other hand, when  $\tau$  is below  $\tau^s$ , two spots approach the peanut shape, but the middle part decays and breaks up into two counter-propagating traveling spots. Those unstable steady states are numerically confirmed and play the role of scattor similar to the 1D case; in fact, we can obtain those unstable steady states by the Newton method and then compute the spectrum after linearization around them. The peanut scattor has five unstable eigenvalues besides the two translation zero eigenvalues, and the largest one ( $\lambda_1 = 0.6275$ ) is much bigger than the others and dominates the dynamics around the peanut scattor. In view of the profile of the associated eigenfunction  $\phi_1$  (Figure 10(B)(a)), it is responsible for merging and pinching off in the middle part of the peanut scattor. On the other hand, the single-horn scattor has two unstable eigenvalues ( $\lambda_1 = \lambda_2 = 0.0921$ ) besides the translation zero eigenvalues, which corresponds to the drift instabilities in 2D. Their eigenfunctions (Figure 10(B)(b)) are basically the same up to rotation. One may think that head-on collisions are rare in higher-dimensional space; however, most of the qualitative changes like annihilation or coalescence occur when one spot runs (almost) straight into the other. Analysis of head-on collisions is a key to understanding the global dynamics. For more detailed discussions, see [17], [18], [19], [26] and the references therein.

## 6. DISCUSSIONS AND OPEN PROBLEMS

The understanding of transient dynamics such as self-replication, self-destruction and scattering among particle-like patterns is a key to clarifying the mechanism

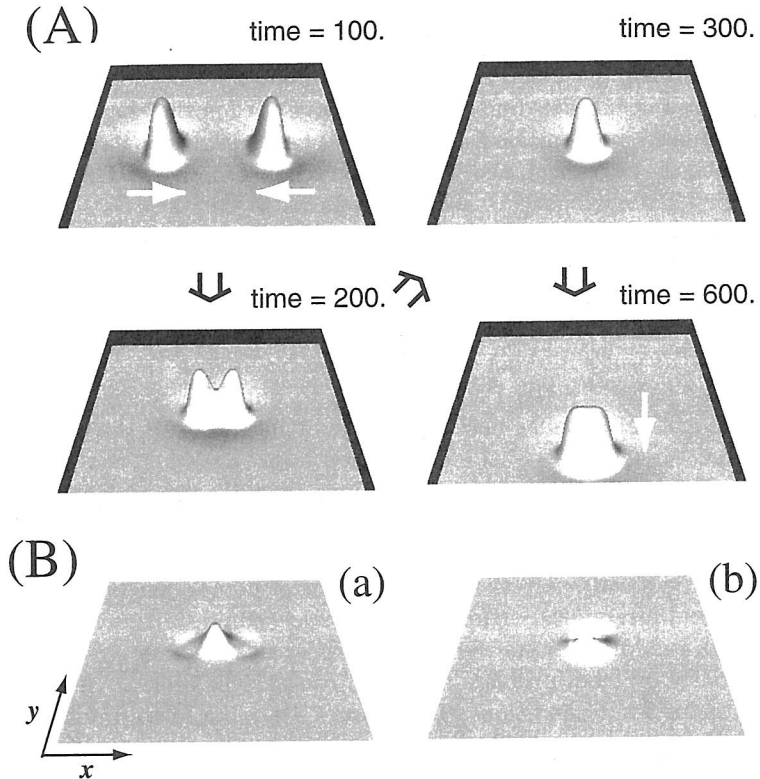


FIGURE 10. (A) Scattering of traveling spots (only  $u$ -component is shown). (B) Profiles of the unstable eigenfunction  $\phi_1$  for the largest eigenvalue: (a) peanut scattor, (b) single-horn scattor, respectively.

for creating complex spatio-temporal patterns in dissipative systems. The topics covered in the previous sections have remained as fertile ground and are waiting for cultivation. Most of the model systems arising in far-from-equilibrium are non-variational, and conventional comparisons and asymptotic methods are not strong enough to obtain satisfactory results on transient dynamics. The computational approach seems to be indispensable for exploring the vivid dynamics and detecting the mathematical mechanisms producing it. What is employed here is a path-continuation method of global solution branches with the aid of AUTO software [2]. This can be used even to tracking 2D patterns for reaction-diffusion systems (see, for instance, [19]). One of the great advantages of this approach is that it allows us to detect in principle all the relevant unstable patterns, although it becomes in general a tough computation for the PDE case. Note that this fits our purpose quite well, since what is needed here is not a stable object but an unstable one like scattor for the collision problem. The computational approach does not directly give us rigorous proof, however.

- It tells us what kind of rigorous mathematical statement is plausible.

- It gives us an overview image of the problem under consideration and suggests to which part a rigorous computer-assisted proof is possible.

The steadily increasing use and power of the computer strengthens our imagination for the dynamics in infinite-dimensional space. On the other hand, there is great potential for many mathematical ideas, which can reveal new aspects of complex dynamics when they are combined with computational methods. One good example is computational homology [11], which allows us to compute various topological quantities and sheds a new light on many practical problems.

The edge splitting discussed in §3 is an example of the first category. Numerical simulation (see Figure 5) shows that only pulses located at an edge can split; however, it does not indicate the underlying mechanism causing such dynamics. It turns out that the pulse-interaction method combined with the saddle-node structure enables us to reduce the PDE dynamics to finite-dimensional systems. The existence of a critical distance necessary for splitting is one of the consequences of this reduction.

The information coming from computational results suggests many interesting problems. For instance, in §4, it is crucial to know the locations of three singularities: saddle-node point of single standing pulse, minimum of saddle-node points for spatially periodic steady states, and Hopf point of homogeneous state, to predict the onset of spatio-temporal chaos. Each location could be computed rigorously; however, it is not known how they are related to each other in a deeper sense. This is obviously a global problem and hard to study in general. A slightly easier question is under what conditions global issues are reduced to unfolding of singularities of high codimension. This is equivalent to finding an organizing center to create a similar dynamics in a miniature sense. Overall it is a key to clarifying the interrelation between local and global properties and understanding the whole dynamics.

#### ACKNOWLEDGEMENTS

The author thanks Shin-Ichiro Ei, Takashi Teramoto, Kei-Ichi Ueda, and Daishin Ueyama for their valuable insights and comments through the discussions.

#### REFERENCES

- [1] M. Bode, A. W. Liehr, C. P. Schenk and H.-G. Purwins, *Interaction of dissipative solitons: Particle-like behaviour of localized structures in a three-component reaction-diffusion system*, Physica D, 161 (2002) 45-66. MR1889807 (2003c:35078a)
- [2] E.J. Doedel, A.R. Champneys, T.F. Fairgrieve, Y.A. Kuznetsov, B. Sandstede and X. Wang, *AUTO97: Continuation and bifurcation software for ordinary differential equations (with HomCont)*, ftp://ftp.cs.concordia.ca/pub/doedel/auto,(1997).
- [3] C. Elphick, E. Meron, and E. A. Spiegel, *Spatiotemporal complexity in traveling patterns*, Phys. Rev. Lett., 61 (1988) 496-499. MR961040 (89g:58150)
- [4] C. Elphick, E. Meron, and E. A. Spiegel, *Patterns of propagating pulses*, SIAM J. Appl. Math. 50 (1990) 490-503. MR1043598 (91k:35033)
- [5] P. Gray and S. K. Scott, *Autocatalytic reactions in the isothermal, continuous stirred tank reactor: Oscillations and instabilities in the system  $A + 2B \rightarrow 3B$ ,  $B \rightarrow C$* , Chem. Eng. Sci. Vol. 39 (1984) 1087-1097.
- [6] S.-I. Ei, *The motion of weakly interacting pulses in reaction-diffusion systems*, J. Dynamic. Diff. Eqs. 14(2002)85-137. MR1878646 (2002m:35117)
- [7] S.-I. Ei, M. Mimura and M. Nagayama, *Pulse-pulse interaction in reaction-diffusion systems*, Physica D, 165 (2002) 176-198. MR1910294 (2003e:35147)

- [8] S.-I. Ei, M. Mimura and M. Nagayama, *Dynamics of spot-solutions in reaction diffusion systems in two dimensional space*, preprint.
- [9] S.-I. Ei, Y. Nishiura and K.-I. Ueda, *2<sup>n</sup>-splitting or edge-splitting? A Manner of splitting in dissipative systems*, Japan J. Indust. Appl. Math. 18 (2) (2001) 181-205. MR1842907 (2002j:35167)
- [10] Y. Hayase and T. Ohta, *Sierpinski Gasket in a Reaction-Diffusion System*, Phys. Rev. Lett. 81 (8) (1998) 1726.
- [11] T. Kaczynski, K. Mischaikow, and M. Mrozek, *Computational Homology*, Springer (2004). MR2028588 (2005g:55001)
- [12] S. Kawaguchi and M. Mimura, *Collision of traveling waves in a reaction-diffusion system with global coupling effect*, SIAM J. Appl. Math. 59 (1999) 920-941. MR1663210 (99j:35105)
- [13] K. Krischer and A. Mikhailov, *Bifurcation to traveling spots in reaction-diffusion systems*, Phys. Rev. Lett. 73 (1994) 3165-3168.
- [14] K. J. Lee, W. D. McCormick, J. E. Pearson, and H. L. Swinney, *Experimental observation of self-replicating spots in a reaction-diffusion system*, Nature 369 (1994) 215-218.
- [15] Y. Nishiura and D. Ueyama, *A skeleton structure of self-replicating dynamics*, Physica D, 130 (1999) 73-104.
- [16] Y. Nishiura and D. Ueyama, *Spatio-temporal chaos for the Gray-Scott model*, Physica D 150 (2001) 137-162.
- [17] Y. Nishiura, K.-I. Ueda and T. Teramoto, *Scattering and separators in dissipative systems*, Phys. Rev. E, 67 (2003) 056210.
- [18] Y. Nishiura, K.-I. Ueda and T. Teramoto, *Dynamic transitions through scatters in dissipative systems*, Chaos, 13 (2003) 962-972.
- [19] Y. Nishiura, K.-I. Ueda and T. Teramoto, *Scattering of traveling spots in dissipative systems*, Chaos 15 (2005) 047509-047519. MR2194913 (2006h:92002)
- [20] Y. Nishiura, *Nonlinear problems I. Mathematics of Pattern Formation Theory (in Japanese)* Iwanami Syoten (1999).
- [21] Y. Nishiura, *Far-from-equilibrium dynamics*, AMS, (2002). MR1903642 (2003g:82059)
- [22] Y. Nishiura, *Dynamics of Self-replication and Self-destruction in Dissipative Systems (in Japanese)*, Iwanami Syoten (2003).
- [23] T. Ohta, *Physics of Non-equilibrium Systems (in Japanese)*, Syokabo (2000).
- [24] J. E. Pearson, *Complex patterns in a simple system*, Science Vol. 216 (1993), 189-192.
- [25] C. P. Schenk, M. Or-Guil, M. Bode and H.-G. Purwins, *Interacting pulses in three-component reaction-diffusion systems on two-dimensional domains*, Phys. Rev. Lett. 78 (1997) 3781-3784.
- [26] T. Teramoto, K. Ueda and Y. Nishiura: *Phase-dependent output of scattering process for traveling breathers*, Phys. Rev. E, 69 (4), (2004) 056224-056232. MR2096551 (2005k:35386)

Translated by YASUMASA NISHIURA

LABORATORY OF NONLINEAR STUDIES AND COMPUTATION, RESEARCH INSTITUTE FOR ELECTRONIC SCIENCE, HOKKAIDO UNIVERSITY, SAPPORO 060-0812, JAPAN